AD-A097 734 SPIRE CORP BEDFORD MA F/G 20/9
TECHNIQUES FOR THE SIMULATION OF THE SPACE PLASMA ENVIRONMENT,(U)
SEP 80 W D HALVERSON F19628-80-C-0055
UNCLASSIFIED SAR-FR-80-60024 AFGL-TR-80-0337 NL

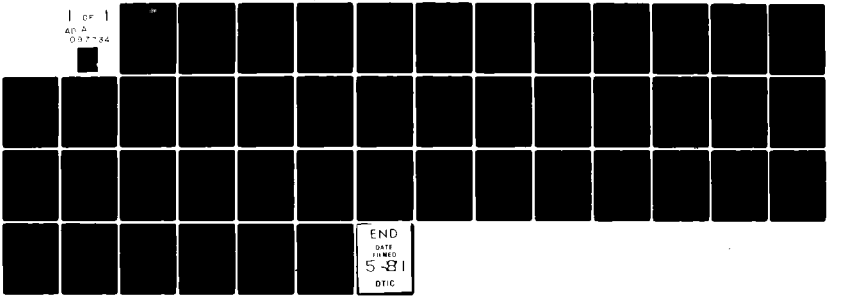

AFGL-TR-80-0337

LEVEL III

12

TECHNIQUES FOR THE SIMULATION OF THE SPACE PLASMA ENVIRONMENT

AD90022

Ward D. Halverson

Spire Corporation
Patriots Park
Bedford, Massachusetts 01730

Scientific Report No. 2

September 1980

AIR FORCE GEOPHYSICS LABORATORY
AIR FORCE SYSTEMS COMMAND
UNITED STATES AIR FORCE
HANSCOM AFB, MASSACHUSETTS 01731

Unclassified

SECURITY CLASSIFICATION OF THIS PAGE (When Data Entered)

REPORT DOCUMENTATION PAGE	READ INSTRUCTIONS BEFORE COMPLETING FORM
1. REPORT NUMBER: AFGL-TR-80-0337	2. GOVT ACCESSION NO.: AD-A097 734
4. TITLE (and Subtitle): TECHNIQUES FOR THE SIMULATION OF THE SPACE PLASMA ENVIRONMENT	5. TYPE OF REPORT & PERIOD COVERED: Scientific Report No. 2
	6. PERFORMING ORG. REPORT NUMBER: FR-80-60024
7. AUTHOR(s): Ward D. Halverson	8. CONTRACT OR GRANT NUMBER(s): F19628-80-C-0055
9. PERFORMING ORGANIZATION NAME AND ADDRESS: Spire Corporation, Patriots Park, Bedford, MA 01730	10. PROGRAM ELEMENT, PROJECT, TASK AREA & WORK UNIT NUMBERS: 62101F, 7661 08AE
11. CONTROLLING OFFICE NAME AND ADDRESS: Air Force Geophysics Laboratory, Hanscom Air Force Base, Massachusetts 01731, Monitor/A.H. Wendel/PHG	12. REPORT DATE: September 1980
	13. NUMBER OF PAGES: 46
14. MONITORING AGENCY NAME & ADDRESS (if different from Controlling Office)	15. SECURITY CLASS. (of this report): Unclassified
	15a. DECLASSIFICATION DOWNGRADING SCHEDULE

16. DISTRIBUTION STATEMENT (of this Report)

Approved for public release; distribution unlimited.

17. DISTRIBUTION STATEMENT (of the abstract entered in Block 20, if different from Report)

18. SUPPLEMENTARY NOTES

19. KEY WORDS (Continue on reverse side if necessary and identify by block number)

Spacecraft charging, laboratory simulation, electron and ion beams

20. ABSTRACT (Continue on reverse side if necessary and identify by block number)

The effects of space plasmas with distributed spectra of particle energies can be simulated in the laboratory by combinations of monoenergetic electron and ion beams. The energy and current density of beams are calculated to provide piecewise reproduction of distributed spectra and by matching various moments of the velocity distribution functions of space plasmas. Analytical solutions for several cases have been found to simulate Maxwellian and two-Maxwellian distribution functions. Spacecraft charging by geomagnetic

DD FORM 1473 EDITION OF 1 NOV 65 IS OBSOLETE

Unclassified

20. (Continued)

substorm plasmas and combinations of monoenergetic beams is compared qualitatively using a simple model. We find similar charging characteristics for the plasmas and a few beams specified by the moment matching techniques.

FOREWORD

The author gratefully acknowledges the significant contributions to the work reported here by Betty A. Reid, Stephen N. Bunker and Steven H. Face.

TABLE OF CONTENTS

LIST OF FIGURES

LIST OF TABLES

SECTION 1
INTRODUCTION

Interactions between the plasmas in space and the surface and various subsystems of spacecraft are very complicated and have been the subject of considerable study over the past several years. Electrostatic charging,[1,2,3] for example, of a spacecraft's surface can result in discharges which can cause electromagnetic interference, degradation of surface materials, and failures of sensitive components. Techniques to influence plasma-spacecraft interactions, such as on-board plasma generators and conductive coatings for dielectrics, are also being actively studied.[3]

The plasma environment of space can be partially simulated in the laboratory using low-temperature plasma generators for studies of phenomena in the ionosphere and low-earth-orbit or combinations of electron and ion beams to simulate the conditions in high-altitude orbits. Several small space plasma simulation laboratories[e.g., 4] and a few large-scale facilities are in operation[5] or being planned.[6] Laboratory simulation, however, is necessarily only a partial re-creation of the actual environment to which a spacecraft is subjected.

The selection of the plasma generators or beams to simulate the space environment is now based on intuitive as well as scientific, engineering, and economic grounds. The simulation often represents only the most extreme case expected for a given spacecraft component. There are presently no established techniques for selecting a laboratory plasma environment to simulate the measured or postulated properties of plasmas in space.

The object of this work is to investigate some mathematical techniques which could be used to choose the parameters of monoenergetic beams to simulate space plasmas. The moderate temperature plasmas of geomagnetic substorms serve as examples for simulation, since they are known to cause electrostatic charging on geosynchronous satellites. The multikiloelectronvolt energies and densities of a few particles per cubic centimeter require their simulation by monoenergetic beams rather than by low-energy plasmas with a continuous energy spectrum.

SECTION 2
BEAM SELECTION TECHNIQUES

2.1 GENERAL

The plasma environment of space is characterized by a wide variety of particle energies, fluxes, species, and spectral shapes. The particle spectra vary with position in space, time, and solar activity. Models of the environment have been developed in various degrees of complexity, ranging from the definition of average plasma properties such as density and temperature at a given altitude to presentations of detailed spectra of "typical" plasma injection events recorded by instrumented satellites.

A space simulation facility is necessarily limited by engineering considerations to providing a few charged particle beams to simulate spacecraft-environment interactions. Presently, the parameters of the electron and ion sources are selected to provide only a rough simulation of the plasma environment. The energy and current densities provided are often chosen to represent the most extreme case envisioned for a given spacecraft or component. Apparently, no quantitative techniques now exist to measure the "quality" of a beam simulation; and no methodology has been developed to specify the number, relative current densities, and relative energies of a set of charged particle beams designed to simulate a given plasma spectrum.

In this section we examine techniques which can be used to specify the parameters of multiple monoenergetic charged particle beams which would provide a mathematically correct and physically plausible simulation of a given plasma environment. The techniques are based on the piecewise reproduction of the shape of distributed energy spectra or by matching various averages of the velocity distribution functions by the monoenergetic beams.

In this study we assume that the space plasma to be simulated is of high enough energy and low enough density so that collective effects in the plasma can be neglected. More precisely, the Debye length of the plasma is considerably greater than typical dimensions of a spacecraft. This assumption is justified for the space environment outside the plasmasphere during geomagnetic substorms when strong spacecraft charging events are recorded.

2.2 PIECEWISE SPECTRAL REPRODUCTION

The simplest and most obvious method to simulate a distributed spectrum is to break the spectrum into several bands and provide monoenergetic beams with appropriate currents and energies to reproduce the distribution in a "piecewise" manner. A very close reproduction of the distributed spectrum can be made in this way, provided there is a sufficient number of available beams.

With a limited number of beams, a problem arises on the choice of the energy boundaries between the parts of the spectrum to be simulated. Possible choices include fractions or multiples of the average energy (temperature) or velocity, or boundaries which divide the particle flux into equal fractions of the total flux. A given spectrum may also be divided to account for particular features, such as a high energy "tail" of the distribution function.

The principles involved in piecewise spectral reproduction can be illustrated by considering a Maxwellian distribution of particle energies,

$$f(E) = \frac{2n}{\sqrt{\pi}} (kT)^{-3/2} E^{1/2} \exp\left(-\frac{E}{kT}\right) \tag{2-1}$$

where n is the number density, kT is the temperature, and E is the kinetic energy of the particles.

The differential energy spectrum of current density crossing an arbitrary surface is given by

$$\frac{dj}{dE} = j_o \frac{E}{(kT)^2} \exp\left(-\frac{E}{kT}\right) \tag{2-2}$$

where

$$j_o = \frac{qn}{4} \left(\frac{8}{\pi} \frac{kT}{m}\right)^{1/2} \tag{2-3}$$

is the total current density; q and m are the charge and mass of the particles.

Integrating Eq. (2-2) over a range of energy bounded by E_1 and E_2, we find

$$j(E_1,E_2) = j_o \left[\left(1 + \frac{E_1}{kT}\right) e^{-\frac{E_1}{kT}} - \left(1 + \frac{E_2}{kT}\right) e^{-\frac{E_2}{kT}}\right] \tag{2-4}$$

This current density must be supplied by a monoenergetic beam with an energy between E_1 and E_2 to simulate the corresponding part of the distributed spectrum. The energy of the beam can be chosen in a number of ways; a relatively simple choice is to use the value found by averaging over the differential energy spectrum of the current density.

$$\bar{E}(E_1,E_2) = \frac{\int_{E_1}^{E_2} E \frac{dj}{dE} dE}{j(E_1,E_2)} \tag{2-5}$$

Integration of Eq. (2-5) gives,

$$\bar{E}(E_1,E_2) = \frac{j_o T}{j(E_1,E_2)} \left\{ \left[\left(1 + \frac{kT}{E_1} \right)^2 + 1 \right] e^{-\frac{E_1}{kT}} - \left[\left(1 + \frac{kT}{E_2} \right)^2 + 1 \right] e^{-\frac{E_2}{kT}} \right\} \tag{2-6}$$

Table 2-1 gives values for $j(E_1,E_2)/j_o$ and $E(E_1,E_2)$ for the case of a 10 keV Maxwellian spectrum divided into four ranges of energy with boundaries at 0, 7.5, 15, and 30 keV.

TABLE 2-1. PIECEWISE REPRODUCTION OF MAXWELLIAN SPECTRUM BY FOUR BEAMS

Maxwellian Temperature = 10 keV

Energy Boundaries E_1,E_2 (keV)	Normalized Current Density $j(E_1,E_2)/j_o$	Beam Energy $E(E_1,E_2)$ (keV)
0, 7.5	0.173	4.682
7.5, 15	0.269	11.20
15, 30	0.359	21.49
30	0.199	42.53

2.3 MOMENT-MATCHING TECHNIQUES

2.3.1 Velocity Moments

A plasma can be characterized by various averages of the velocity distributions of its constituent particles. In general, the "velocity moments" of a given distribution function, f(v), are defined by

$$M_k = 4\pi \int_0^\infty v^k \, f(v) \, v^2 dv \qquad k = 0,1,2,\text{----}. \tag{2-7}$$

where the $4\pi v^2 dv$ term represents an infinitesimal element in (isotropic) velocity space.

The velocity moments, M_k, can be related to physical averages for several values of k. For example, M_0, M_1, M_2, and M_3 are related, respectively, to the average number density $\langle N \rangle$, particle flux, $\langle NF \rangle$, pressure, $\langle P \rangle$, and energy flux, $\langle EF \rangle$, of the given particle type in the plasma.

$$M_0 = \langle N \rangle = n \tag{2-8}$$

$$M_1 = 4\pi \langle NF \rangle = n \langle v \rangle = n \left(\frac{8}{\pi} \frac{kT}{m} \right)^{1/2} \tag{2-9}$$

$$M_2 = \frac{3}{m} \langle P \rangle = \frac{3\pi}{8} n \left(\frac{8}{\pi} \frac{kT}{m} \right)^{1} \tag{2-10}$$

$$M_3 = \frac{8\pi}{m} \langle EF \rangle = \frac{\pi}{2} n \left(\frac{8}{\pi} \frac{kT}{m} \right)^{3/2} \tag{2-11}$$

$$M_4 = \frac{15}{64} \pi^2 n \left(\frac{8}{\pi} \frac{kT}{m} \right)^{2} \tag{2-12}$$

$$M_5 = \frac{3}{8} \pi^2 n \left(\frac{8}{\pi} \frac{kT}{m} \right)^{5/2} \tag{2-13}$$

The average speed, $\langle v \rangle$, in Equation 2-9 is defined by

$$\langle v \rangle = \frac{M_1}{M_0} \tag{2-14}$$

The expressions on the right-hand side of Equations (2-8) - (2-13) are given for the case of a Maxwellian velocity distribution,

$$f(v) = n \left(\frac{m}{2\pi kT}\right)^{3/2} e^{-\frac{mv^2}{2kT}} \tag{2-15}$$

where n, m, and T are respectively the number density, mass, and temperature of the particles and k is Boltzmann's constant.

Average and RMS "Temperatures"

A useful method for characterizing a non-Maxwellian plasma is to define effective temperatures which are related to ratios of the velocity moments.[7] The average and RMS temperatures are given by

$$T_{AV} = \frac{1}{k} \frac{\langle P \rangle}{\langle N \rangle} = \frac{m}{3k} \frac{M_2}{M_0} \tag{2-16}$$

$$T_{RMS} = \frac{1}{k} \frac{\langle P \rangle}{2\langle N \rangle} = \frac{m}{4k} \frac{M_3}{M_1} \tag{2-17}$$

The two temperatures are equal when the velocity distribution is Maxwellian.

2.3.2 *Monoenergetic Beams to Match Velocity Moments*

A technique to simulate a plasma with a distributed velocity distribution is to choose the velocities and particle densities of monoenergetic beams so that their velocity moments match those of the plasma. Under these conditions, the average parameters of the beams, such as number density, pressure, or energy flux, are equal to those of the plasma component under simulation.

In general, a single beam can match two moments of the distributed spectrum, so that two beams can match four moments, three beams, six moments, etc. As discussed in Section 2.3.4, it is also possible to overspecify the problem and use more than the minimum number of beams to match a given number of velocity moments.

Single Beam Energy

A monoenergetic beam can match two moments according to the simultaneous equations,

$$\begin{aligned} n_b v_b^{\,j} &= M_j \\ n_b v_b^{\,k} &= M_k \end{aligned} \qquad (j \neq k) \tag{2-18}$$

where n_b and v_b are the density and velocity of the beam particles.

For example, when the zeroth (number density) and second (pressure) moments are chosen,

$$n_b = n$$

$$v_b = \left(\frac{M_2}{M_0}\right)^{1/2} = \left(\frac{3\ k\ T_{AV}}{m}\right)^{1/2} \tag{2-19}$$

or, in terms, of beam energy, E_b,

$$E_b = \frac{3}{2}\ k\ T_{AV} \tag{2-20}$$

If the first (number flux) and third (energy flux) moments are used,

$$n_b = \frac{M_1}{v_b} = n\ \langle v \rangle \left(\frac{m}{4\ kT_{RMS}}\right)^{1/2}$$

$$v_b = \left(\frac{M_3}{M_1}\right)^{1/2} = \left(\frac{4\ kT_{RMS}}{m}\right)^{1/2} \tag{2-21}$$

or

$$E_b = 2\ k\ T_{RMS} \tag{2-22}$$

Two Beam Energies

The densities and velocities of two monoenergetic beams can be found to match the zeroth through third velocity moments of the distributed spectrum by solving four simultaneous equations:

$$\begin{aligned} n_1 + n_2 &= n \\ n_1 v_1 + n_2 v_2 &= n \langle v \rangle \\ n_1 v_1^2 + n_2 v_2^2 &= \frac{3}{m} n\ T_{AV} \\ n_1 v_1^3 + n_2 v_2^3 &= \frac{4}{m} n \langle v \rangle\ T_{RMS} \end{aligned} \tag{2-23}$$

where n_1, n_2, v_1, and v_2 are the densities and velocities of the beams, and the velocity moments of the distributed spectrum have been replaced by relations (2-14), (2-16), and (2-17). Boltzmann's constant, k, has been taken to be unity.

It is shown in Appendix A that the velocities and densities of the monoenergetic beams can be found analytically.

$$v_{1,2} = \frac{\langle v \rangle}{6\ T_{AV} - 2\ m \langle v \rangle^2} \left\{ 4\ T_{RMS} - 3\ T_{AV} \right.$$
$$\left. \pm \left[8\ T_{RMS} \left(2\ T_{RMS} - 9\ T_{AV} + 2\ m \langle v \rangle^2 \right) - 27\ T_{AV}^2 \left(1 - \frac{4\ T_{AV}}{m \langle v \rangle^2} \right) \right]^{1/2} \right\} \tag{2-24}$$

$$n_1 = n\left(\frac{v_2 - \langle v \rangle}{v_1 - v_2}\right)$$
$$n_2 = n - n_1 \tag{2-25}$$

For a Maxwellian plasma, where $T_{AV} = T_{RMS} = T$, Eq. (2-24) simplifies somewhat,

$$v_{1,2} = \frac{\pi}{6\pi - 16}\langle v \rangle \left\{1 \pm \left(\frac{27}{2}\pi + \frac{128}{\pi} - 83\right)^{1/2}\right\} \tag{2-26}$$

The beam densities and energies are then found to be

$$n_1 = 0.382\ n$$
$$n_2 = 0.618\ n \tag{2-27}$$

$$E_1 = 3.007\ T$$
$$E_2 = 0.568\ T \tag{2-28}$$

Three Beam Energies

Six moments of the distributed spectrum can be used to compute the densities and velocities of three monoenergetic beams. No analytical solutions have been found for this case, but iterative techniques can be used to find solutions of the set of six simultaneous, nonlinear equations.

As discussed in Appendix B, the beam velocities and densities can be found in terms of the average speed and density of the plasma particles. For the case of a Maxwellian plasma with temperature, T, the beam densities and energies are

$$n_{1,2,3} = [0.087,\ 0.588,\ 0.325]\ n$$
$$E_{1,2,3} = [4.931,\ 1.657,\ 0.303]\ T \tag{2-29}$$

Different values will be found for other types of velocity distribution functions, but the method used to compute the Maxwellian results is general for all realistic spectral shapes.

2.3.3 Two-Maxwellian Plasmas

Garrett showed that a two-Maxwellian fit is often a good representation of plasma distribution functions measured during geomagnetic substorms.[8] The density and temperature of each Maxwellian component can be found from four velocity moments of the measured spectrum. It is possible, in principle, to find three-Maxwellian fits which match six moments, although the effects of errors in measurement of the plasma spectrum become increasingly exaggerated when computing the high-order moments. It should also be possible to find multiple-Maxwellian least-square fits directly from the measured distribution functions without computing the velocity moments of the data.

Single Beam Energy

A two-Maxwellian distribution has average and RMS temperatures given by

$$T_{AV} = \frac{n_1 T_1 + n_2 T_2}{n_1 + n_2} \tag{2-30}$$

$$T_{RMS} = \frac{n_1 T_1^{3/2} + n_2 T_2^{3/2}}{n_1 T_1^{1/2} + n_2 T_2^{1/2}} \tag{2-31}$$

where n_1, n_2, T_1, and T_2 are the respective densities and temperatures of the two components of the spectrum.

A single monoenergetic beam can match two velocity moments of the distributed spectrum if its density and energy are chosen according to Eqs. (2-19) - (2-22) above. For example, if the beam density is equal to the total plasma density, $n_1 + n_2$, and its energy is 3/2 T_{AV}, then the zeroth and second velocity moments of the two-Maxwellian plasma and the monoenergetic beam are equal.

Two Beam Energies

Two methods exist for matching the velocity moments of a two-Maxwellian distribution by two monoenergetic beams. First, the energy and density of each beam can be chosen individually to match two moments of each of the Maxwellian components of the spectrum. In this case, Eqs. (2-19)-(2-22) would be employed along with the densities and temperatures of the two-Maxwellian fit.

The second approach is to use the average and RMS temperatures of the two-Maxwellian fit, Eqs. (2-30) and (2-31), and to calculate the beam velocities and densities from Eqs. (2-24) and (2-25). In both cases, as many as four moments of the two-Maxwellian distribution function can be matched by two monoenergetic beams. In practical situations, physical considerations would be required to make a choice between the two methods of matching velocity moments.

Three or More Beam Energies

The moments of a two-Maxwellian distribution function can be matched in several different combinations with multiple monoenergetic beams. As in the two-beam case, each Maxwellian component of the plasma can have one or more beams assigned to it which individually match velocity moments. For six-moment matching, three beam energies and densities could be selected using Eq. (2-29) for each component, and a total of six beam energies would be required to simulate the two-Maxwellian plasma. As mentioned above, the computed values of the zeroth through fifth moment of the full spectrum can also be used directly to find three beam energies and densities through the iterative minimization procedure described in Appendix B.

2.3.4 Arbitrarily Assigned Beam Energies

The velocity moments of a measured distribution function can also be matched by monoenergetic beams whose velocities are chosen arbitrarily. As an example, four monoenergetic beams can match four velocity moments:

$$\begin{aligned} n_1 + n_2 + n_3 + n_4 &= M_0 \\ v_1 n_1 + v_2 n_2 + v_3 n_3 + v_4 n_4 &= M_1 \\ v_1^2 n_1 + v_2^2 n_2 + v_3^2 n_3 + v_4^2 n_4 &= M_2 \\ v_1^3 n_1 + v_2^3 n_2 + v_3^3 n_3 + v_4^3 n_4 &= M_3 \end{aligned} \qquad (2\text{-}32)$$

When the four beam velocities are fixed, then it is only a matter of solving a set of linear simultaneous equations for the beam densities, n_1 through n_4. It should be pointed out that not all combinations of beam velocity may be chosen for v_1 through v_4, because negative, and therefore unphysical, solutions for the beam densities can be obtained in some cases.

Table 2-2 gives the densities calculated for three, four, and five beams as a function of preassigned beam energies. The beam energies and densities are normalized to the temperature and density of a Maxwellian distribution, and the velocity moments used for the calculations are given by the right-hand side of Eqs. (2-8)-(2-12). The first three-beam solution in Table 2-2 is a check of the six-moment solution, Eq. (2-29), found by the iterative procedure discussed in Section 2.3.2.

Table 2-2 indicates that, although the velocity moments of the monoenergetic beams are matched, the spectral shape of the beam solutions is generally not similar to that of a Maxwellian. For a simulation facility one would intuitively prefer an envelope of the beam density which roughly approximates the Maxwellian distribution, Eq. 2-1. The low and negative values of density found for some combinations of beam energy apparently result from forcing the beam densities alone to bring about the match between the velocity moments. The unphysical and intuitively unsatisfying results using arbitrarily assigned beam energies cast doubt on the usefulness of this approach to match velocity moments of distributed spectra.

TABLE 2-2. PARTICLE DENSITIES FOR PREASSIGNED BEAM ENERGIES

No. of Beams	E_j/kT	n_j/n
3	0.303	0.325
	1.657	0.588
	4.931	0.087
3	0.5	0.521
	2.0	0.339
	4.0	0.140
4	0.4	0.282
	0.8	0.333
	1.6	0.069
	3.2	0.316
4	0.5	0.518
	1.5	0.156
	2.5	0.134
	3.5	0.192
5	0.2	0.198
	0.6	0.061
	1.3	0.548
	3.0	0.127
	5.0	0.066
5	0.2	0.179
	0.6	0.162
	1.5	0.502
	3.0	0.086
	5.0	0.071

SECTION 3
SPACECRAFT CHARGING CALCULATIONS

3.1 RATIONALE

The previous section presented some mathematical techniques to relate the characteristics of undisturbed plasmas to those of one or more monoenergetic beams of charged particles. It was assumed that the plasma or beams produced a flux of particles at a given surface, although no interactions between the particles and the surface were considered.

In this section we shall compare the electrostatic charging produced by plasmas and various combinations of monoenergetic electron and ion beams using a model which accounts for several of the interactions between the incident charged particles and a "typical" spacecraft. The spacecraft charging calculations are, of course, only one of several possible approaches for making a qualitative comparison of the effects of plasmas and combinations of monoenergetic beams. A spacecraft simulation facility, however, will devote a considerable amount of its effort to the study of the effects of electrostatic charging, and this choice for comparison can be justified on these grounds.

3.2 CHARGING MODEL

The spacecraft charging model developed by Garrett[9] calculates the equilibrium potential of a surface which receives isotropic fluxes of electrons and ions with arbitrary energy spectra and which loses charge by secondary electron emission, electron backscatter, and photoelectric emission. The model has been rather successful in predicting the potential of high-altitude satellites instrumented to measure the differential energy spectra of electrons and protons in geomagnetic substorm plasmas[10].

The model assumes that the spacecraft can be represented as a spherical Langmuir probe in a plasma whose Debye length is much greater than the dimensions of the probe. The energy spectra of the plasma electrons and ions are divided into 62 energy "bins", and the flux of charged particles to the surface calculated, taking into account the electrostatic potential of the satellite and conservation of mass. Maxwellian, two Maxwellian, and arbitrary spectra observed from the spacecraft's instrumentation can be loaded into the energy bins.

Secondary electron emission from electron and ion bombardment and electron backscatter are calculated as a function of the incident particle flux and the measured energy dependence of the secondary emission and backscatter coefficients of aluminum. Corrections for the heterogeneous surface of an actual spacecraft are made by small adjustments of these coefficients to bring the calculated potential of the satellite equal to its measured value when the satellite is in "typical" plasma conditions. Charge losses by photoemission are included by an empirical formula.

We have modified the model in two ways. First, the time dependence of charging was included by representing the satellite as an isolated spherical capacitor. The amount of charge gained and lost by the surface is calculated for short increments of time in which the potential is held constant. The net gain of charge is then used to compute the new value of potential to be used during the following time increment. This procedure is repeated until the potential of the model satellite does not vary in succeeding increments of time.

The second modification was used only for potential calculations of the model when irradiated by monoenergetic, initially parallel beams of noninteracting charged particles. It accounts for the electrostatic deflection of the beams in the electric field of the charged body which attracts oppositely charged particles and repels particles of the same sign.

The total current to a surface of arbitrary shape in a parallel beam is simply the product of the current density, j, and the geometric cross section, A, in a plane perpendicular to the current density vector. If the initially parallel beam is deflected by a symmetrical potential well, the deflection can be represented as an "effective" cross-sectional area which depends on the strength of the field and the kinetic energy and charge of the particles. It is shown in Appendix C that the effective area of a spherical conductor of radius R is,

$$A_{eff} = \pi R^2 \left(1 - \frac{q\varphi_s}{|qE|}\right) \qquad (q\varphi_s < |qE|)$$
$$A_{eff} = 0 \qquad (q\varphi_s > |qE|) \qquad (3\text{-}1)$$

where φ_s is the (signed) potential of the sphere, and q and E are the (signed) charge and initial kinetic energy of the incident charged particles.

For the charging calculations, the electron and ion current to the model satellite was set equal to the sum of the currents from the monoenergetic beams, each of which was given by

$$I_i = j_i A_{eff} \tag{3-2}$$

where j_i is the unperturbed current density of the i^{th} beam with energy E_i.

The secondary emission current from electron and ion bombardment and the electron backscattering were calculated as a function of the energy of the incident particles by the same subroutines used by Garrett's model for distributed energy spectra.

No photoemission was included in the spacecraft charging calculations in order to simplify comparison of the results between monoenergetic beams and distributed spectra.

3.3 RESULTS

The spacecraft charging model was used to calculate the potential of a spherical satellite with a radius of 1 meter and initial potential of zero. The charging by plasmas with several different electron and ion temperatures were compared to charging by beams whose energies and current densities were selected by the methods discussed in Section 2. Table 3-1 presents the parameters of some of the Maxwellian plasmas and beams and for the charging calculations.

3.3.1 Single Monoenergetic Beams and Maxwellian Plasmas

Charging by monoenergetic electron and proton beams and Maxwellian plasma was computed for several beam energies and plasma temperatures. The current densities and energies were selected so that the first (number flux) and third (energy flux) velocity moments of the monoenergetic beams matched those of the Maxwellian plasmas, Equations (2-21) and (2-22). For this case, the beam energies were twice the corresponding plasma temperature.

$$E_b = 2kT$$

$$I_b = qn\sqrt{\frac{kT}{2\pi m}} \tag{3-3}$$

TABLE 3-1. SPACECRAFT CHARGING BY MAXWELLIAN PLASMAS AND MONOENERGETIC BEAMS

PLASMA		
Electrons:	T_e = 10 keV, j_e = 1.0 nA/cm^2	φ_{eq} = -12.5 kV
Ions:	T_i = 10 keV, j_i = 0.023 nA/cm^2	
Electrons:	T_e = 10 keV, j_e = 1.0 nA/cm^2	φ_{eq} = -14.2 kV
Ions:	T_i = 20 keV, j_i = 0.033 nA/cm^2	
BEAMS		
1 Electron:	E_e = 20 keV j_e = nA/cm^2	φ_{eq} = -13.5 kV
1 Ion:	E_i = 20 keV j_i = 0.023 nA/cm^2	
1 Electron:	E_e = 20 keV j_e = 1.0 nA/cm^2	φ_{eq} = -12.9 kV
1 Ion:	E_i = 40 keV j_i = 0.033 nA/cm^2	
2 Electron:	E_{e1} = 5.69 keV j_{e2} = 0.41 nA/cm^2 E_{e2} = 30.1 keV j_{e2} = 0.59 nA/cm^2	φ_{eq} = -15.0 kV
2 Ion:	E_{i1} = 5.69 keV j_{i1} = 0.0096 nA/cm^2 E_{i2} = 30.1 keV j_{i2} = 0.014 nA/cm^2	

TABLE 3-1. (Concluded)

3 Electron:	E_{e1} = 3.03 keV	
	j_{e1} = 0.16 nA/cm^2	
	E_{e2} = 16.6 keV	
	j_{e2} = 0.67 nA/cm^2	
	E_{e3} = 49.6 keV	
	j_{e3} = 0.17	φ_{eq} = -11.9 kV
3 Ion:	E_{i1} = 3.03 keV	
	j_{i1} = 0.0037 nA/cm^2	
	E_{i2} = 16.57 keV	
	j_{i2} = 0.016 nA/cm^2	
	E_{i3} = 49.6 keV	
	j_{i3} = 0.0040 nA/cm^2	

where n and T are the density and temperature of the Maxwellian plasma component, q and m are the charge and mass of the plasma and beam particles (assumed the same species), and E_b and j_b are the undisturbed energy and current density of the beam.

Figure 3-1 shows the charging of the model satellite with a radius of 1 meter under irradiation by single 20 keV electron and proton beams and by a hydrogen plasma in which the electron and ion temperatures are 10 keV. It can be seen that the charging rate and equilibrium potential of the satellite is higher when exposed to the monoenergetic beams, although some differences are to be expected because of the important influence of the secondary electron emission coefficients on the charging process.

The equilibrium potentials found from calculations of charging by Maxwellian plasma and beams with energies and current densities given by Equation (3-3) are compared in Figure 3-2. The correspondence is surprisingly good, considering the crudeness of simulating a Maxwellian velocity distribution by a single monoenergetic beam.

Figure 3-3 shows calculations of charging by a Maxwellian plasma with an electron temperature of 10 keV and an ion (proton) temperature of 20 keV. Charging by electron beams with an energy of 20 keV and proton beams of 40 keV and current densities for each component given by Equation (3-3) are also shown. In this case, the equilibrium potential in the Maxwellian plasma is somewhat higher than under irradiation by the beams.

3.3.2 Two Monoenergetic Beams and Maxwellian Plasma

The energies and densities required for two beams to match four velocity moments of a Maxwellian plasma are given in Equations (2-27) and (2-28). We have calculated the charging by two electron and proton beams and in Maxwellian plasmas.

Figure 3-4 shows the results of the calculations for electron and ion beams with energies of 5.69 keV and 30.1 keV and for a Maxwellian plasma with electron and ion temperatures of 10 keV. The equilibrium potential of the satellite model is more than 2 kV greater for charging by the beams than by the plasma, although the charging rate is about equal for both cases for 0 to 0.05 seconds.

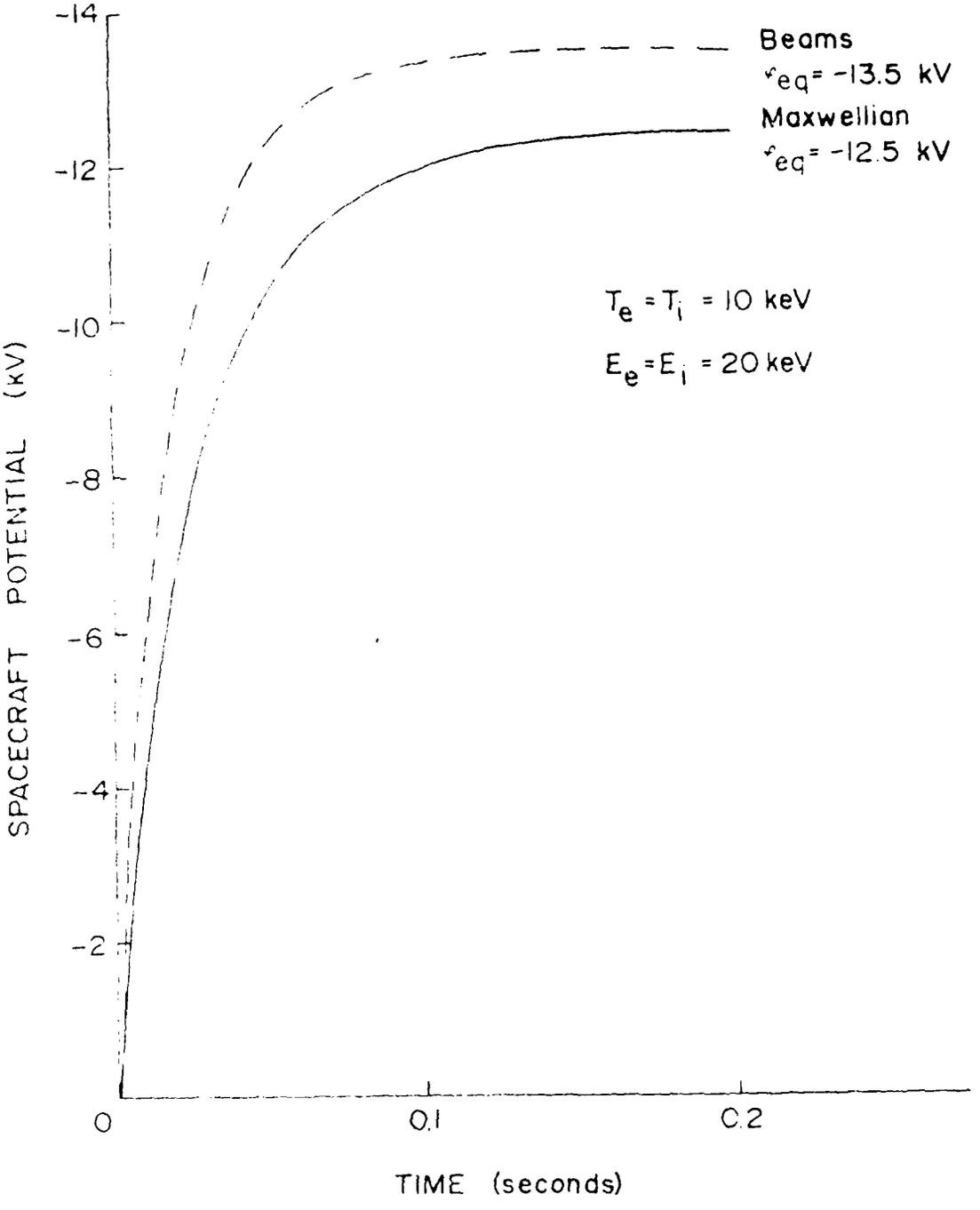

FIGURE 1. SPACECRAFT CHARGING BY 10 keV MAXWELLIAN PLASMA AND 20 keV ELECTRON AND ION BEAMS

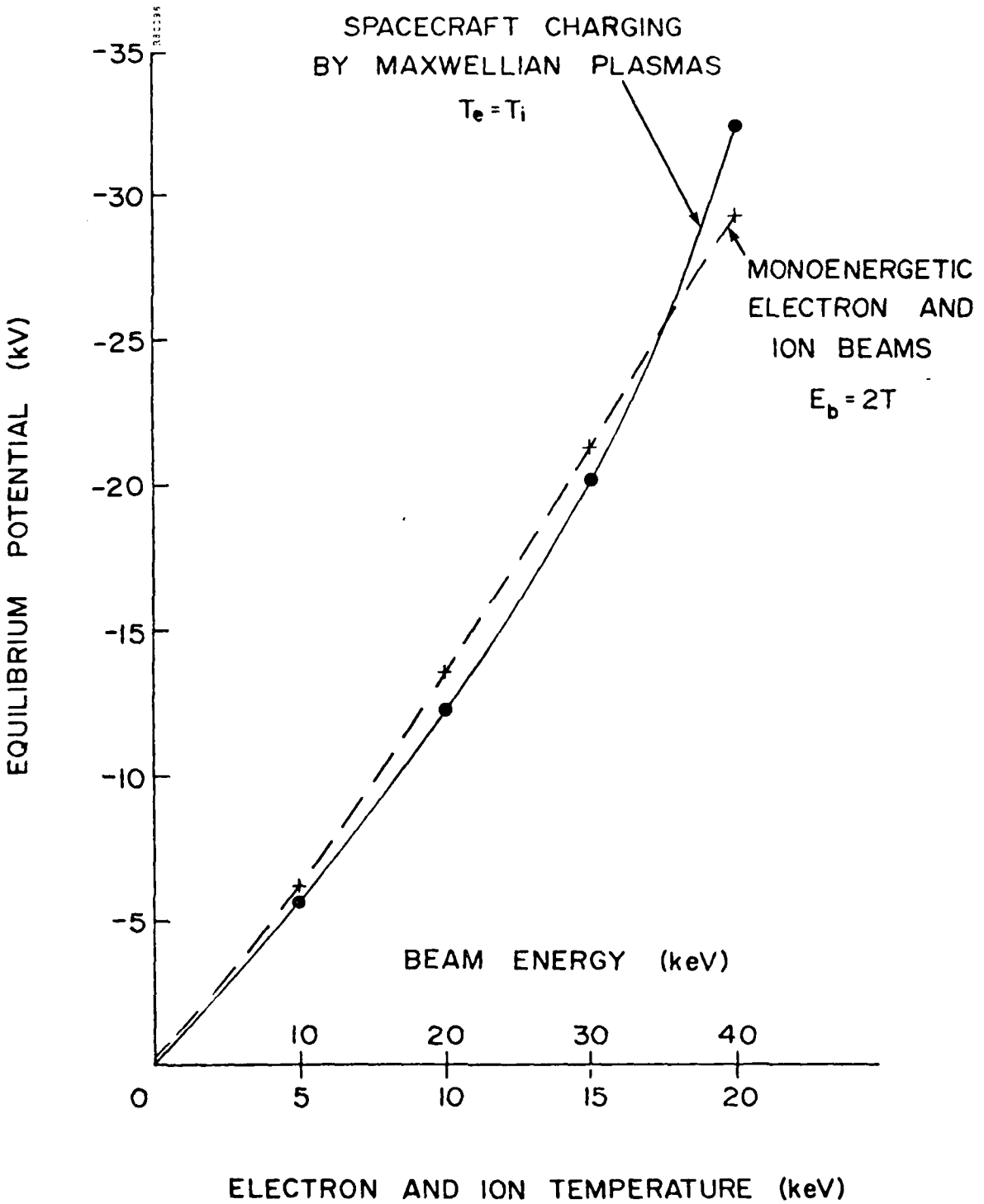

FIGURE 3-2. EQUILIBRIUM POTENTIAL IN MAXWELLIAN PLASMAS AND SINGLE ELECTRON AND ION BEAMS

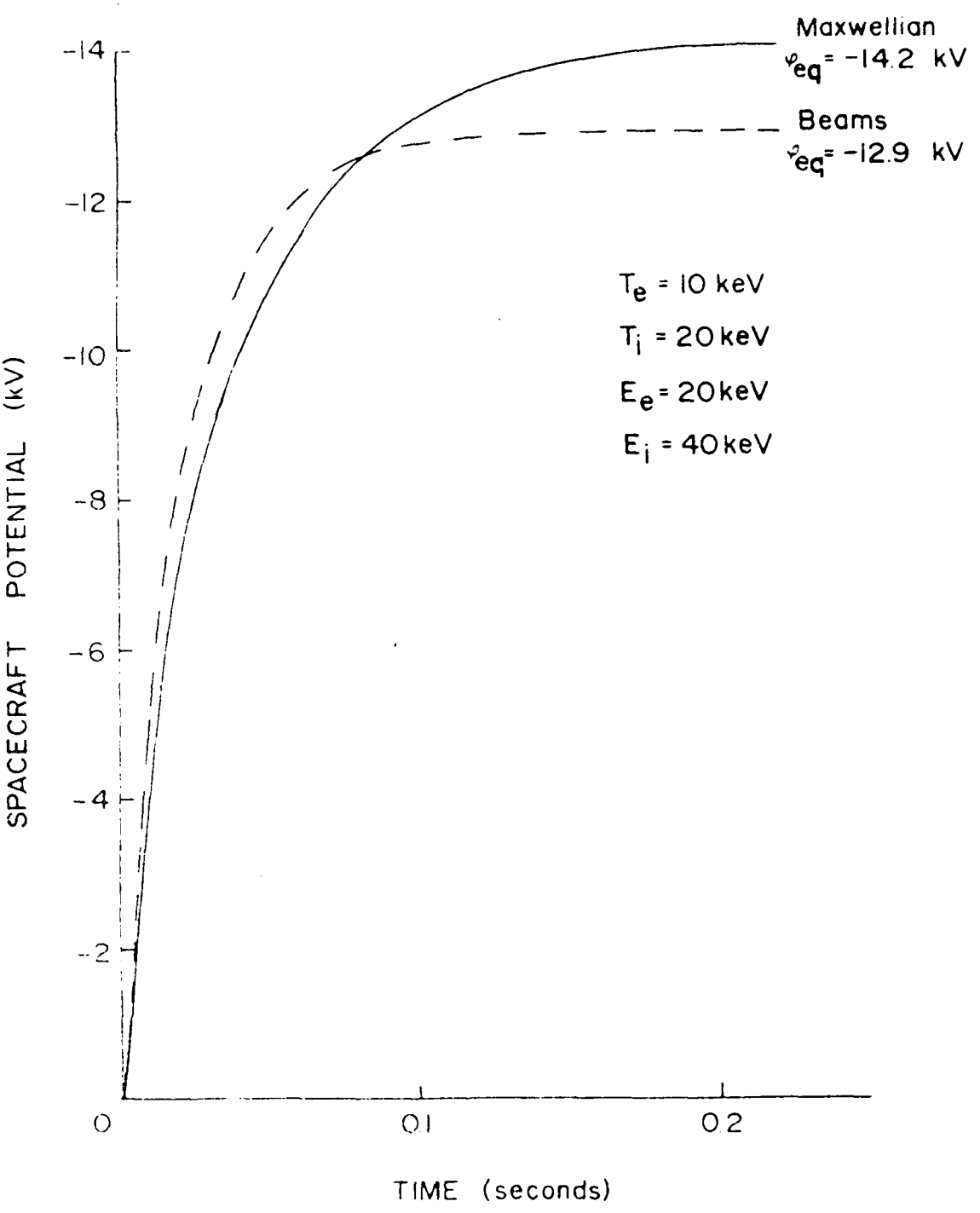

FIGURE 3-3. CHARGING BY MAXWELLIAN PLASMA (T_e = 10 keV, T_i = 20 keV) AND SINGLE ELECTRON AND ION BEAMS

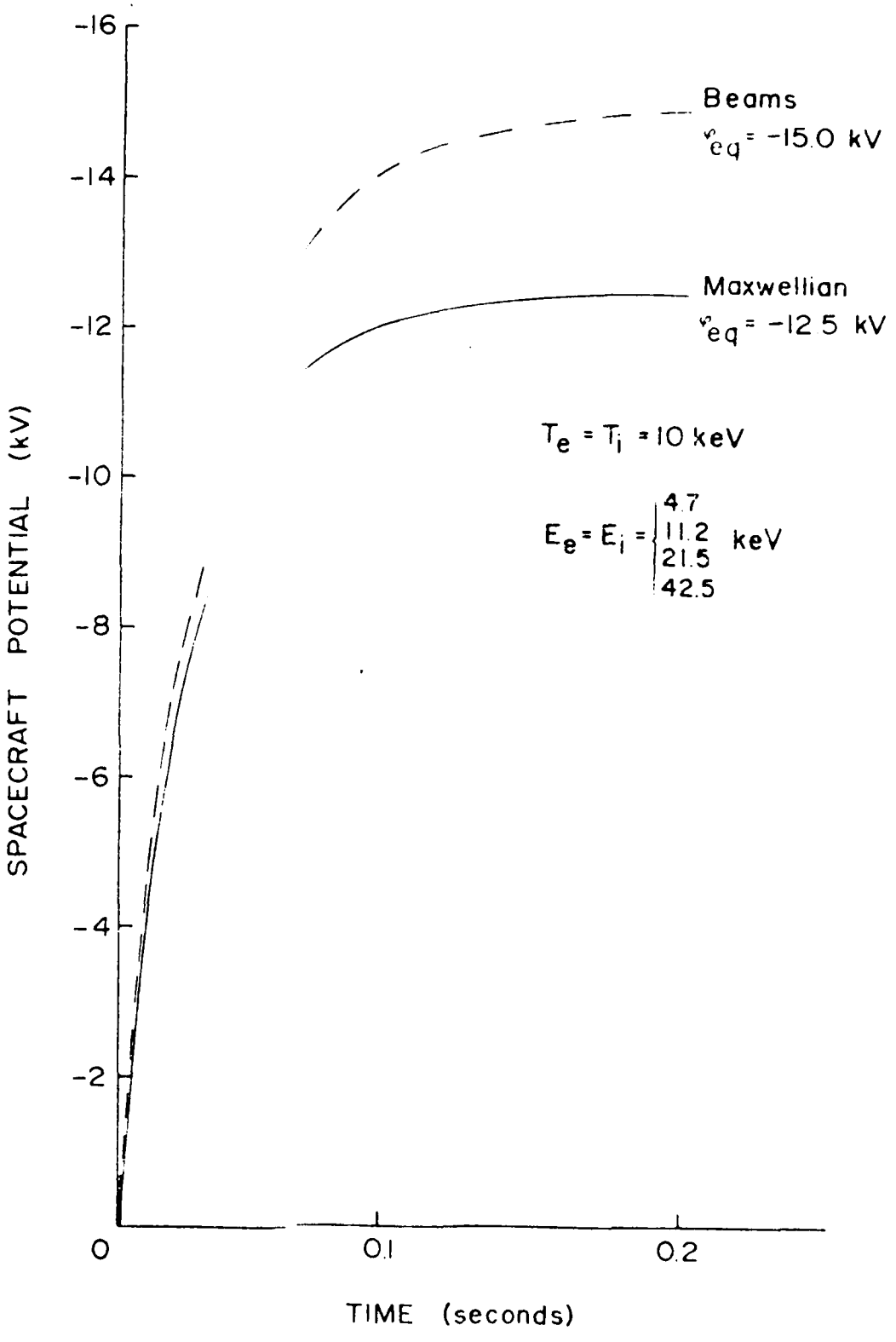

FIGURE 3-4. CHARGING BY MAXWELLIAN PLASMA AND TWO ELECTRON AND ION BEAMS

3.3.3 Three Monoenergetic Beams and Maxwellian Plasma

Charging by three monoenergetic electron and three monoenergetic electron and ion beams whose velocity moments match six moments of a Maxwellian plasma was computed using the spacecraft charging model. The beam energies and currents were found from Equations (2-29) to match the velocity moments of a Maxwellian hydrogen plasma with an electron and ion temperature of 10 keV.

The results of the charging calculations are shown in Figure 3-5. There is very close agreement between the charging rates and equilibrium potentials for both the three-beam and Maxwellian plasma cases.

3.3.4 Four Beams and Maxwellian Plasma

The charging of the satellite model was calculated using beams chosen to simulate the differential energy spectrum of the current density of a Maxwellian plasma. As discussed in Section 2.2, the energy distribution was broken into four parts and the current density and average energy of each part computed, using Equations (2-4) and (2-6).

Figure 3-6 shows the charging using the four-beam solution given in Table 2-1 compared with charging by a Maxwellian plasma with electron and ion temperatures of 10 keV. It is somewhat surprising that the equilibrium potential found with four electron and ion beams chosen to mimic the spectral shape of the Maxwellian plasma is not as close as with other cases with fewer beams.

3.3.5 Beams and Two-Maxwellian Plasma

As discussed in Section 2.3.3, the velocity distribution of a non-Maxwellian plasma can be approximated by a two-Maxwellian distribution function, each component of the distribution being characterized by a temperature and a particle density. We have computed the charging of the satellite model in a plasma with a two-Maxwellian electron distribution function and single-Maxwellian ions. The two electron components have temperatures of 10 keV and 30 keV, and densities of 3.0 cm^{-3} and 0.43 cm^{-3}, respectively. The proton plasma has a temperature of 10 keV and has a number density equal to the total electron density.

We have compared the charging by the two-Maxwellian plasma to that of several combinations of monoenergetic beams. Table 3-2 shows the beam energies, current densities, and resultant equilibrium potential of the satellite model.

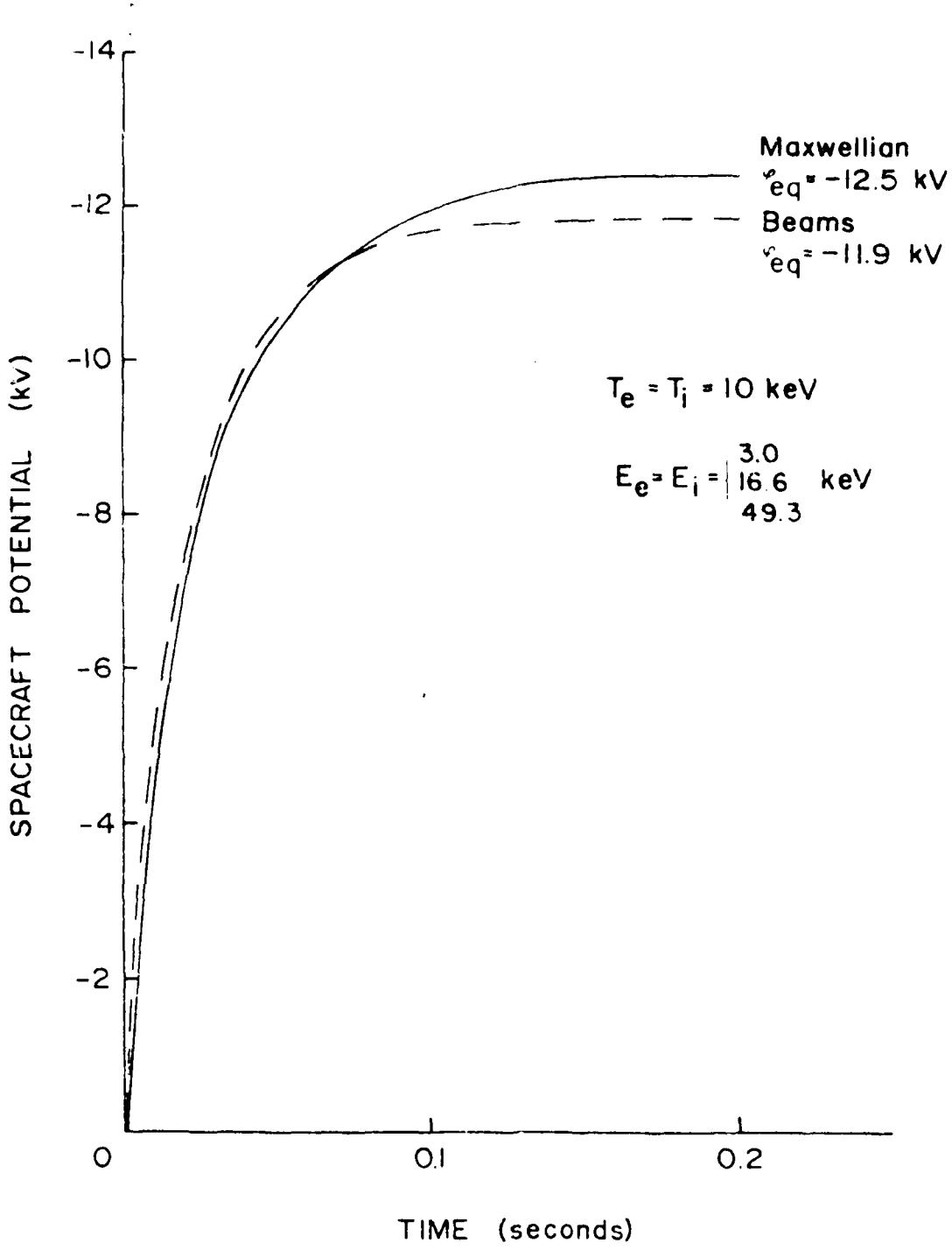

FIGURE 3-5. CHARGING BY MAXWELLIAN PLASMA AND THREE ELECTRON AND ION BEAMS

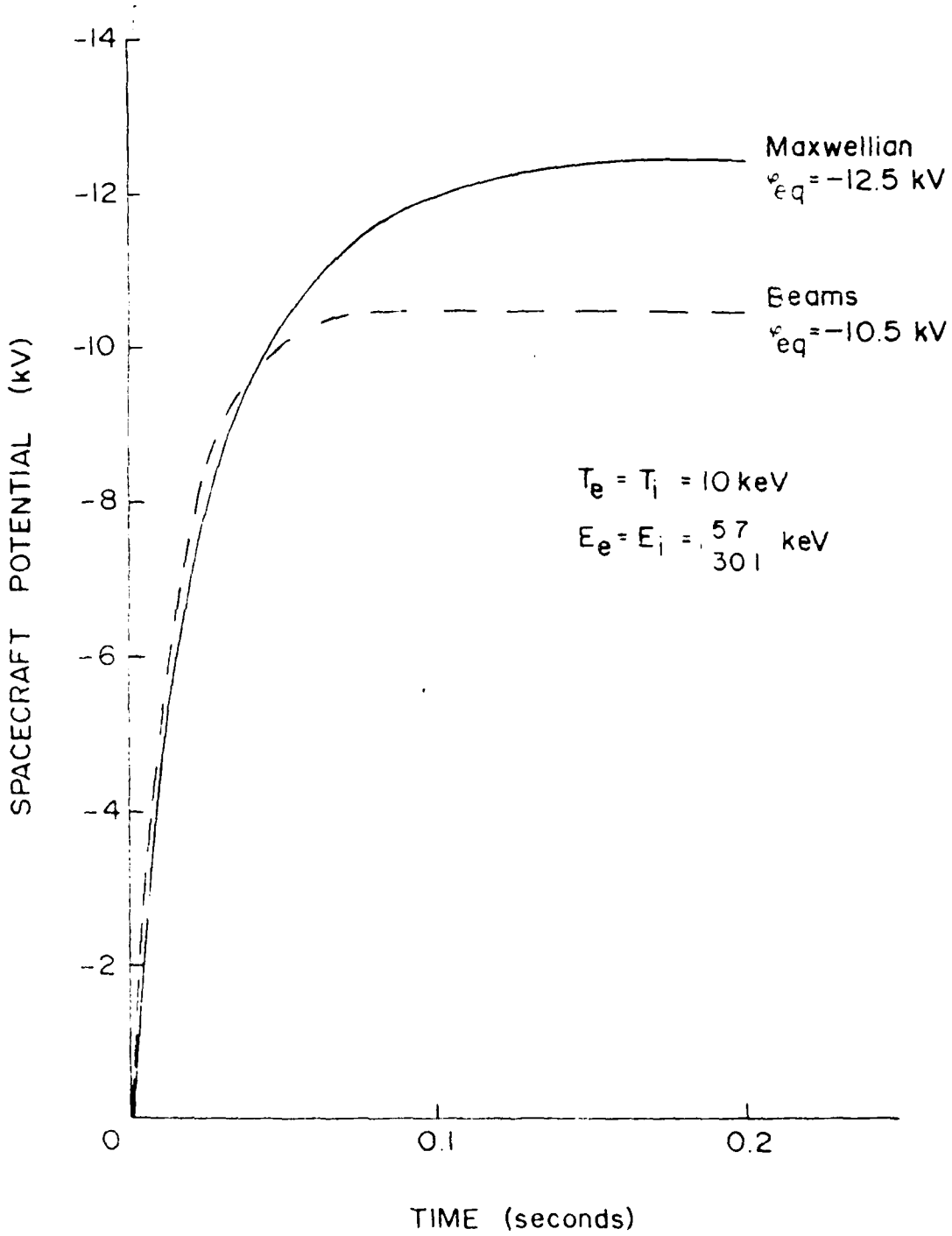

FIGURE 3.6. CHARGING BY MAXWELLIAN PLASMA AND FOUR ELECTRON AND ION BEAMS

TABLE 3-2. SPACECRAFT CHARGING BY TWO-MAXWELLIAN PLASMA AND MONOENERGETIC BEAMS

PLASMA		
Electrons:	T_{e1} = 10 keV, j_{e1} = 0.8 nA/cm^2 T_{e2} = 30 keV, j_{e2} = 0.2 nA/cm^2 $(T_e)_{AV}$ = 12.52 keV $(T_e)_{RMS}$ = 14.0 keV	φ_{eq} = -14.0 kV
Ions:	T_i = 10 keV, j_i = 0.021 nA/cm^2	
BEAMS		
1 Electron	$E_e = 2(T_e)_{RMS}$ = 28.0 keV	φ_{eq} = -26.8 kV
1 Electron	E_e = 3/2 $(T_e)_{AV}$ = 18.8 keV j_e = 1.1 nA/cm^2	φ_{eq} = -12.7 kV
1 Ion	E_i = 3/2 T_i = 15 keV j_i = 0.023 nA/cm^2	
1 Electron	$E_e = 2(T_e)_{RMS}$ = 28.0 keV j_e = 1.0 nA/cm^2	φ_{eq} = -19.8 kV
1 Ion	E_i = 2 T_i = 20 keV j_i = 0.021 nA/cm^2	
2 Electron	E_{e1} = 2 T_{e1} = 20 keV j_{e1} = 0.8 nA/cm^2 E_{e2} = 2 T_{e2} = 60 keV j_{e2} = 0.2 nA/cm^2	φ_{eq} = -18.2 kV
1 Ion	E_i = 2 T_i = 20 keV j_i = 0.021 nA/cm^2	
2 Electron	E_{e1} = 7.92 keV, j_{e1} = 0.54 nA/cm^2 E_{e2} = 51.9 keV, j_{e2} = 0.46 nA/cm^2	φ_{eq} = -19.2 kV
2 Ion	E_{i1} = 5.69 keV, j_{i1} = 0.0096 nA/cm^2 E_{i2} = 30.07 keV, j_{i2} = 0.014 nA/cm^2	

The equilibrium potential found with a single electron beam is presented to show the effect of removing ions from the simulation. Without the ion component, the satellite model charges until the secondary electron emission and backscatter are equal to the incident electron flux. The equilibrium potential is close to that of the electron beam because the secondary electron emission coefficient peaks at an energy of a few hundred electronvolts[9] and is small at higher energies.

The single-electron and single-ion beam energies and currents in Table 3-2 were chosen to match two velocity moments of the two-Maxwellian plasma, as discussed in Section 2.3.2. The two-electron and single-ion beam energies and currents match the first and third velocity moments (particle and energy flux) of each component of the distribution functions.

The energies and currents of the two-electron and two-ion beam case were found, using Equations (2-24) and (2-25), to match four velocity moments of the distribution functions, based on the average and RMS temperatures of the plasma particles.

The discrepancies between the calculations of equilibrium potential in the two-Maxwellian plasma and in monoenergetic beams are somewhat greater than those found with a single Maxwellian plasma. The difference may be caused by the higher temperature component of the electron plasma, which skews the second and third velocity moments of the electron distribution function. The high-energy electron beams required to match these velocity moments apparently have a strong influence on the equilibrium potential of the model.

3.4 DISCUSSION

The calculations give a qualitative idea of the charging which would be observed in a spacecraft testing facility in which monoenergetic beams were used to simulate space plasmas with distributed energy spectra. As expected, the equilibrium potential of the spacecraft under test, and therefore the charge density on its surface, is only a function of the electron and ion beam energies and currents. An important result, however, is the observation that the monoenergetic beams can be chosen to match several velocity moments of a distributed spectrum and, at the same time, produce the same charge density on the spacecraft. Thus, surface phenomena which are influenced, for example, by energy flux as well as charge density can be investigated in a laboratory facility with a reasonable degree of confidence in the simulation fidelity.

It should be made clear that the charging model used here is a very simple one and does not account for the complex geometry or surface details of a real spacecraft. More complicated charging codes exist, however, which could be used to make more detailed comparisons of spacecraft charging by monoenergetic beams and space plasmas. The NASCAP code[11], for example, is probably the most ambitious attempt to represent the geometrical and surface configuration of real satellites in the environment of geosynchronous orbit. Modifications of NASCAP would be required to calculate the charging of a three-dimensional object under irradiation by beams of charged particles,[12] but it is likely that NASCAP would be a useful tool for comparing the conditions of laboratory simulation to those of space.

SECTION 4
SUMMARY AND RECOMMENDATIONS

4.1 SUMMARY

We have examined mathematical techniques to choose the energy and current density of monoenergetic beams to simulate the distributed spectra of plasmas in space. In the first approach, the differential current density spectrum of the plasma was divided into a number of energy bands. The beam energy and current were calculated for each band to provide a piecewise reproduction of the distributed spectrum. This technique is probably the most intuitively satisfying when a large number of beams with different energies can be used for the simulation because the envelope of the velocity distribution of the beams can closely mimic that of the plasma.

The second general approach was to choose the beam energies and current densities to match the velocity moments of the plasma distribution function. The velocity moments are averages related to physical quantities such as particle density, flux, pressure, and energy flux, and have been used extensively to characterize the measured properties of plasmas in space. We have found expressions for beam energies and densities in terms of the plasma properties such as the average and RMS "temperature", density, and average velocity. Combinations of one, two, and three beams were found to match two to six velocity moments of Maxwellian distributions. The same techniques also can be applied to other spectral shapes, and they were used to examine two-Maxwellian distributions. Unphysical or intuitively unsatisfying results were found when the problem was overspecified by arbitrarily selecting beam energies and beam densities calculated to match a set of velocity moments of a distributed spectrum.

A simple computational model was used to compare the charging of a spacecraft by plasmas with distributed spectra and by monoenergetic beams. The plasmas were similar to those found in high orbits during geomagnetic substorms, with multikilovolt temperatures and a few particles per cubic centimeter. These calculations were made to gain a qualitative comparison of the approaches for choosing monoenergetic beams to simulate space plasmas.

Although a close comparison was not expected when only a few beams were used to simulate the distributed spectrum of a plasma, some combinations of beams gave similar charging rates and equilibrium potentials. The equilibrium potentials found using beams to match velocity moments of a two-Maxwellian plasma generally

were within a few kilovolts of charging by the distributed spectrum, but showed more divergence than the simulations of simple Maxwellian plasmas. The spacecraft charging model cannot be used as the only criterion to evaluate the fidelity of simulation of a given plasma environment, because physical considerations other than the charging rate and equilibrium potential must also be considered in this evaluation.

4.2 RECOMMENDATIONS

A number of characteristics of space plasmas have not been included in this analysis which may be important for certain simulation situations. The most evident of these is the observed anisotropy of the velocity distributions of particles in space. Plasma drifts are common as well as distributions which show strong correlations with the direction of the magnetic field in space. Plasmas are often characterized as "drifting Maxwellian", "bi-Maxwellian" (temperature parallel to the magnetic field different from perpendicular), or "loss cone" distributions (very few particles in a cone in velocity space). These anisotropies can be important for interactions with spacecraft with large oriented surfaces or cavities aligned with the directed plasma flux.

We recommend that the present work be extended to account for anisotropies in the velocity distributions in space. A number of techniques exist to describe mathematically the anisotropies, such as expressing the distribution function in terms of spherical harmonics. Some of these techniques can probably be used to provide objective relationships between plasma parameters and the placement of electron and ion sources in a simulation facility.

Except for the calculations of average charging using the simple spacecraft charging model, we have not considered the interactions between the plasma particles and the surface of a spacecraft. In fact, the behavior of a dielectric material irradiated by electrons and ions depends to a large degree on the profile of charged particles trapped in the upper atomic layers of the surface. This profile is a function of the material, particle species, energy distribution, and angle of incidence on the surface. An isotropic plasma with a distributed energy spectrum will produce a very different charging profile from that of a monoenergetic beam.

We recommend that further theoretical and computational studies be performed to illustrate these differences and provide guidelines for the selection of monoenergetic beams to reproduce the charging effects from plasmas in typical spacecraft materials. A number of computer codes exist which, through Monte Carlo routines, follow the trajectories of "typical" energetic particles in materials. They account for deflections by elastic and inelastic collisions and energy losses by the same processes and by radiation. The equilibrium profile of charge in an insulating material can be found by following the trajectories of a few thousand particles and simple models of charged particle mobility in the material. The codes can accept a variety of input conditions, including distributions of particle velocities and incident angles, and can be run on a moderate size computer.

Calculations of the interactions of charged particles with spacecraft materials should be coupled with experimentation to test their validity and verify results and predictions. We recommend that a small-scale experimental program be undertaken to accomplish these ends. Samples of spacecraft material should be simultaneous irradiated by electrons of more than one energy, ions (preferably protons) and light with a strong component in the extreme ultraviolet. The experiments should be performed under very good vacuum conditions to avoid surface contamination by oil or other materials which are atypical of the space environment.

Some experimentation of this type has already been reported by the spacecraft charging scientific community.[e.g., 3] However, the materials were usually irradiated by a single electron beam, and no attempt was made to correlate surface phenomena with theoretical analysis. The fact that no ion beams were included in the tests may also strongly modify the surface interactions in comparison with those in the plasma environment of space.

REFERENCES

1. A. Rosen, editor, Spacecraft Charging by Magnetospheric Plasmas, (M.I.T. Press, Cambridge, Massachusetts, 1975).

2. C.P. Pike and R.R. Lovell, editors, Proc. of the Spacecraft Charging Technology Conference, Report No. AFGL-TR-77-0051, Air Force Geophysics Laboratory, Hanscom AFB, Mass., 1977.

3. R.C. Finke and C.P. Pike, editors, Spacecraft Charging Technology - 1978, NASA Conference Publication 2071, NASA Lewis Research Center, Cleveland, Ohio, 1979.

4. F.D. Berkopec, N. John Stevens, and J.C. Sturman, "The Lewis Research Center Geomagnetic Substorm Simulation Facility", Report No. NASA TM X-73502, NASA Lewis Research Center, Cleveland, Ohio, 1976.

5. O.L. Pearson, "Modification of a Very Large Thermal-Vacuum Test Chamber for Ionosphere and Plasmasphere Simulation", American Institute of Aeronautics and Astronautics, Inc., New York, Paper 78-1625, 1978.

6. W. Halverson, "Modifications of Ionospheric Simulation Capability. Volume 1: Study", Report No. FR-60021, Spire Corporation, Bedford, Massachusetts, 1979.

7. H.B. Garrett, E.G. Mullen, E. Ziemba, and S.E. DeForest, "Modeling of the Geosynchronous Orbit Plasma Environment - Part 2", Report No. AFGL-TR-78-0304, Air Force Geophysics Laboratory, Hanscom AFB, Massachusetts, 1978.

8. H.B. Garrett, "Modeling of the Geosynchronous Orbit Plasma Environment - Part 1", Report No. AFGL-TR-77-0288, Air Force Geophysics Laboratory, Hanscom AFB, Massachusetts, 1977.

9. H.B. Garrett, "Spacecraft Potential Calculations - A Model", Report No. AFGL-TR-78-0116, Air Force Geophysics Laboratory, Hanscom AFB, Mass., 1978.

10. H.B. Garrett and S.E.Deforest, J. Geophys. Res. 84, 2083 (1979).

11. I. Katz, J.J. Cassidy, M.J. Mandell, G.W. Schnuell, P.G. Steen, and J.C. Roche, "The Capabilities of the NASA Charging Analyzer Program", Spacecraft Charging Technology - 1978 (see Ref. 3).

12. J.C. Roche, private communication, 1979.

APPENDIX A

TWO BEAM SOLUTION TO MATCH FOUR VELOCITY MOMENTS

Garrett[1] has shown for a similar problem that the set of nonlinear simultaneous equations, Eq. (17), can be reduced to a single quadratic equation of the form,

$$AX^2 + BX + C = 0 \tag{A-1}$$

where A, B, and C are functions of the right-hand side of Eqs. (17). For the problem of calculating the velocities and densities of monoenergetic beams, we have set

$$\begin{aligned} X &= \frac{v_{1,2}^2}{\langle v \rangle^2} \\ A &= 1 - \frac{3}{m}\frac{T_{AV}}{\langle v \rangle^2} \\ B &= \frac{4}{m}\frac{T_{RMS}}{\langle v \rangle^2} - \frac{3}{m}\frac{T_{AV}}{\langle v \rangle^2} \\ C &= \frac{9}{m^2}\left(\frac{T_{AV}}{\langle v \rangle^2}\right)^2 - \frac{4}{m}\frac{T_{RMS}}{\langle v \rangle^2} \end{aligned} \tag{A-2}$$

The beam velocities are found to be

$$\begin{aligned} v_{1,2}^2 = \frac{\langle v \rangle^2}{6\,T_{AV} - 2\,m\langle v \rangle^2} \cdot \Bigg\{ & 4\,T_{RMS} - 3\,T_{AV} \\ & \pm \Bigg[9\,T_{AV}^2 + 12\,T_{RMS}^2 - 9\,T_{AV}\,(4\,T_{RMS} - m\langle v \rangle^2) \\ & - 27\,T_{AV}^2\left(1 - \frac{4\,T_{AV}}{m\langle v \rangle^2}\right)\Bigg]^{1/2} \Bigg\} \end{aligned} \tag{A-3}$$

where v_1 (v_2) corresponds to the + (-) sign of Eq. (A-3).

The beam densities corresponding to the velocities are found by substitution,

$$n_1 = n\left(\frac{v_2 - \Delta v_2}{v_1 - v_2}\right) \qquad (A\text{-}4)$$

$$n_2 = n - n_1$$

APPENDIX B

THREE-BEAM SOLUTION TO MATCH SIX VELOCITY MOMENTS

To find a three-beam solution to match six velocity moments of a distributed spectrum, six nonlinear simultaneous equations must be solved. These equations are of the form

$$\sum_{k=1}^{3} \sum_{j=0}^{5} n_k v_k^j = M_j \tag{B-1}$$

where n_k and v_k are the densities and velocities of the beams, and M_j represents the j^{th} velocity moment of the distributed spectrum.

Although any physically reasonable distribution function can be utilized, we used the six velocity moments of a Maxwellian distribution, Eqs. (2)-(7), to find solutions of Eq. (B-1). The beam densities and velocities were normalized by changing variables,

$$a,b,c = \frac{n_{1,2,3}}{n} \tag{B-2}$$

$$x,y,z = \frac{v_{1,2,3}}{\langle v \rangle}$$

so that the moment equations for a Maxwellian distribution become

$$\begin{aligned}
&a + b + c = 1 \\
&ax + by + cz = 1 \\
&ax^2 + by^2 + cz^2 = \frac{3\pi}{8} \\
&ax^3 + by^3 + cz^3 = \frac{\pi}{2} \\
&ax^4 + by^4 + cz^4 = \frac{15}{64}\pi^2 \\
&ax^5 + by^5 + cz^5 = \frac{3}{8}\pi^2
\end{aligned} \tag{B-3}$$

Eqs. (B-3) can be solved by an iterative procedure that minimizes the expression represented by the absolute sum of Eqs. B-3. Trial solutions are substituted into a computer program which then converges on the best solution through an iterative process.[B-1]

The only solutions of Eqs. (B-3) found by the iterative routine were permutations of the following:

$$\begin{aligned}(x,y,z) &= (1.9679,\ 1.14085,\ 0.4881)\\ (a,b,c) &= (0.0866,\ 0.5879,\ 0.3255)\end{aligned} \tag{B-4}$$

The energies of the beams were found from

$$E_1 = \frac{4}{a^2 + \ldots^2} \tag{B-5}$$

and similar expressions for E_2 and E_3.

B-1. P.R. Bevington, Data Reduction and Error Analysis for the Physical Sciences (McGraw-Hill Book Company, New York, 1969), Ch. 11.

APPENDIX C
EFFECTIVE AREA OF SPHERICAL CONDUCTOR

We shall assume that a sphere of radius R is in a uniform, parallel beam of non-interacting charged particles of mass, m, and (signed) charge, q. If the sphere is uncharged, the current to the sphere is given by,

$$I(0) = \pi R^2 j_o \tag{C-1}$$

where j_o is the current density of the undisturbed beam.

When the object charges, the particle trajectories of the beam are deflected by the static electric field around the sphere. The effective area of the sphere is then the circular area whose radius is the "impact parameter" of the beam particles that just graze the surface of the sphere.

Elementary texts of classical mechanics show that the impact parameter, b, is related to the distance of closest approach, a, according to the relation,

$$\frac{b^2}{a^2} + \frac{q\varphi(a)}{\frac{1}{2}mv_o^2} = 1 \tag{C-2}$$

The initial kinetic energy of the particles is $1/2mv_o^2$ and $\varphi(a)$ is the electrostatic potential at the distance of closest approach to the sphere. Setting the kinetic energy equal to $|qV_o|$, a = R, the effective area of the sphere is then,

$$A_{eff} = \pi b^2 = \pi R^2\left(1 - \frac{q\varphi_s}{|qV_o|}\right) \quad \left(q\varphi_s < |qV_o|\right) \tag{C-3a}$$

When the potential of the sphere is greater than the initial accelerating voltage of like-signed particles, the particles do not reach the surface.

$$A_{eff} = 0 \quad \left(q\varphi_s < |qV_o|\right) \tag{C-3b}$$

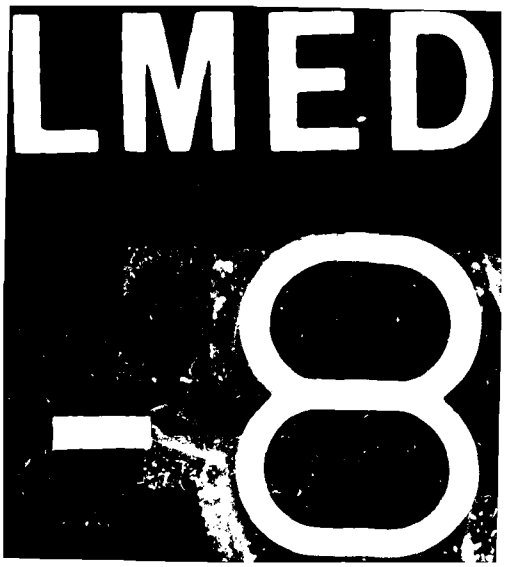
LMED
-8